

# SUPERCONDUCTING ATOMIC CONTACTS AND MULTIPLE ANDREEV REFLECTIONS

J.C. CUEVAS<sup>1</sup>, W. BELZIG<sup>2</sup>

<sup>1</sup>*Institut für Theoretische Festkörperphysik, Universität Karlsruhe, D-76128 Karlsruhe, Germany*

<sup>2</sup>*Department of Physics and Astronomy, University of Basel, Klingelbergstr.82, CH-4056 Basel, Switzerland*

The interplay between experiments on the electronic transport of atomic contacts and recent microscopic theories have consolidated the multiple Andreev reflection as a central concept in mesoscopic superconductivity. Here, we present a theoretical study of the physics of these processes from the point of view of the full counting statistics. We show that the knowledge of this quantity not only allows us to calculate all the transport properties of superconducting point contacts, but also provides an unprecedented level of understanding of this subject.

## 1 Introduction

The current-voltage (I-V) characteristics of superconducting contacts have been the subject of investigation during the last four decades. The first experimental analyses were performed in tunnel junctions. In this case the current inside the superconducting gap is suppressed, and the results can be accurately described with the BCS theory. However, very often a significant current is observed in the subgap region, which cannot be explained with the simple tunnel theory. The first anomalies were reported by Taylor and Burstein<sup>1</sup> who noticed a small onset in the current when the applied voltage  $V$  was equal to the energy gap,  $\Delta/e$ , in a tunneling experiment between two equal superconductors. Soon afterwards it was apparent<sup>2</sup> that not only is there an anomaly in the current at  $eV = \Delta$ , but in fact at all submultiples  $2\Delta/n$ , where  $n$  is an integer. This set of anomalies is referred to as *subharmonic gap structure* (SGS).

The first theoretical attempt to explain the SGS was done by Schrieffer and Wilkins<sup>3</sup>, who noticed that if two electrons could tunnel simultaneously, this process would become energetically possible at  $eV = \Delta$ , and cause the structure in the I-V observed by Taylor and Burstein<sup>1</sup>. Within this *multiparticle tunneling theory* the origin of the SGS would be the occurrence of multiple processes in which  $n$  quasiparticles cross simultaneously the contact barrier. Almost 20 years later, Klapwijk, Blonder and Tinkham<sup>4</sup> introduced the concept of multiple Andreev reflection (MAR) as a possible explanation of the SGS. In this process a quasiparticle undergoes a cascade of Andreev reflections in the contact interface.

The theoretical discussion was finally clarified with the advent of modern mesoscopic theories. Using the scattering formalism<sup>5,6</sup> and the so-called Hamiltonian approach<sup>7</sup>, different authors reported a complete analysis of the dc and ac Josephson effect in point contacts. These theories clearly showed that the MARs are responsible of the subgap transport in these systems. They also showed that the multiparticle tunneling of Schrieffer and Wilkins and the MARs are indeed the same mechanism. The new microscopic theories have also allowed the calculation of a series of properties such as the shot noise<sup>8,9</sup> or the Shapiro steps<sup>10</sup>.

From the experimental point of view, uncertainties in the interface properties have often avoided a sensible comparison between theory and experiment. The situation has considerably improved with the appearance of the metallic atomic-sized contacts, which can be produced by means of scanning tunneling microscope and break-junction techniques<sup>11,12,13,14,15</sup>. These nanowires have turned out to be ideal systems to test the modern transport theories in mesoscopic superconductors. Thus, for instance Scheer and coworkers<sup>12</sup> found a quantitative agreement between the measurements of the current-voltage characteristics of different atomic contacts and the predictions of the theory for a single-channel superconducting contact<sup>6,7</sup>. These

experiments not only helped to clarify the origin of the SGS, but also showed that the set of the transmission coefficients in an atomic-size contact is amenable to measurement. This possibility has recently allowed a set of experiments that confirm the theoretical predictions for transport properties such as supercurrent<sup>14</sup> and noise<sup>15</sup>. From these combined theoretical and experimental efforts a coherent picture of transport in superconducting point contacts has emerged with multiple Andreev reflections (MAR) as a central concept.

The most recent development in the understanding of the dc transport in superconducting contacts is the analysis of the full counting statistics<sup>16,17</sup>. Full counting statistics (FCS) is a familiar concept in quantum optics, which has been recently adapted to electrons in mesoscopic conductors by Levitov and coworkers<sup>18</sup>. FCS gives the probability  $P(N)$  that  $N$  charge carriers pass through a conductor in the measuring time. Once these probabilities are known one can easily compute not only the mean current and noise, but all the cumulants of the current distribution (see Ref. [19]). In Ref. [16] we have demonstrated that the charge transport in superconducting point contacts can be described by multinomial distribution of processes in which a multiple charge is transferred. More importantly, we have shown that the calculation of the FCS allows us to identify the probability of the individual MARs and the charge transferred in these processes. This information probably provides the deepest insight into the transport properties of these systems. In this sense, in this contribution we review of the dc transport properties of superconducting point contacts from the point of view of the FCS approach.

The rest of the paper is organized as follows. In section II, after introducing some basic concepts about charge statistics, we discuss the general result for the FCS of a point contact and we give the expression of the transport properties in terms of the MAR probabilities. Finally, section III is devoted to the application of the general results to the description of the current, noise and third cumulant in superconducting atomic contacts.

## 2 Full counting statistics of multiple Andreev reflections

### 2.1 Some basic concepts

Our goal is to calculate the full counting statistics of a superconducting contact. Thus, the quantity that we are interested in is the probability  $P_{t_0}(N)$ , that  $N$  charges are transferred through the contact in the time interval  $t_0$ . Equivalently, we can find the *cumulant generating function* (CGF)  $S(\chi)$ , which is defined by

$$\exp(S(\chi)) = \sum_N P_{t_0}(N) \exp(iN\chi). \quad (1)$$

Here,  $\chi$  is the so-called counting field. From the knowledge of the CGF one can easily obtain the different cumulants that characterize the probability distribution  $C_n = -(-i)^n (\partial^n S / \partial \chi^n)_{\chi=0}$ . Notice that the first cumulants are related to the moments of the distribution as follows

$$C_1 = \bar{N} \equiv \sum_N N P_{t_0}(N), \quad C_2 = \overline{(N - \bar{N})^2}, \quad C_3 = \overline{(N - \bar{N})^3}, \quad C_4 = \overline{(N - \bar{N})^4} - 3\overline{(N - \bar{N})^2}^2, \quad (2)$$

and so on. It is also important to remark that these cumulants have a simple relation with the relevant transport properties that are actually measured. Thus for instance, the mean current is given by  $I = (e/t_0)C_1$  and the symmetrized zero frequency noise is given by  $S_I = (2e^2/t_0)C_2$ .

### 2.2 Keldysh-Green's function approach to FCS

As mentioned above, our system of interest is a voltage-biased superconducting point contact, i.e. two superconducting electrodes linked by a constriction, which is much shorter than the

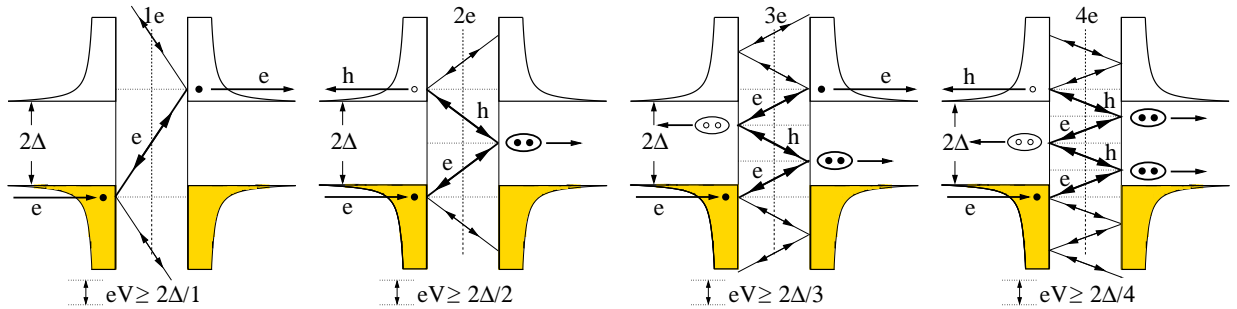


Figure 1: Schematic representation of the MARs for BCS superconductors with gap  $\Delta$ . We have sketched the density of states of both electrodes. In the left panel we describe the process in which a single electron tunnels through the system overcoming the gap due to a voltage  $eV \geq 2\Delta$ . The other panels show MARs of order  $n = 2, 3, 4$ . In these processes an incoming electron at energy  $E$  undergoes at least  $n - 1$  Andreev reflections to finally reach an empty state at energy  $E + neV$ . In these MARs a charge  $ne$  is transferred with a probability, which for low transparencies goes as  $T^n$ . At zero temperature they have a threshold voltage  $eV = 2\Delta/n$ . The arrows pointing to the left in the energy trajectories indicate that a quasiparticle can be normal reflected. The lines at energies below  $E$  and above  $E + neV$  indicate that after a detour a quasiparticle can be backscattered to finally contribute to the MAR of order  $n$ .

superconducting coherence length. We concentrate ourselves in the case of a single channel contact described by a transmission probability  $T$ .

To obtain the FCS in a superconducting point contact we make use of the Keldysh-Green's function approach to FCS introduced by Nazarov and one of the authors<sup>20,21</sup>. As shown in Ref. [16] the CGF for superconducting point contact at finite bias  $V$  has the form

$$S(\chi) = \frac{t_0}{h} \int_0^{eV} dE \ln \left[ 1 + \sum_{n=-\infty}^{\infty} P_n(E, V) (e^{in\chi} - 1) \right]. \quad (3)$$

The different terms in the sum in Eq. (3) correspond to transfers of multiple charge quanta  $ne$  at energy  $E$  with the probability  $P_n(E, V)$ , which can be seen by the  $(2\pi/n)$ -periodicity of the accompanying  $\chi$ -dependent counting factor. This result proves that the charges are indeed transferred in large quanta. Below we find for any kind of superconducting junction explicit expressions for  $P_n(E, V)$ , which is just the probability of a  $n^{\text{th}}$ -order MAR. In this process a quasiparticle injected at energy  $E$  is  $n - 1$  times Andreev reflected to be transmitted at energy  $E + neV$ , resulting in a transfer of  $n$  electron charges. This is illustrated in Fig. 1.

At zero temperature the MAR probabilities  $P_n(E, V)$  can be calculated analytically in terms of the lead Green functions  $g^{R,A}(E)$  and  $f^{R,A}(E)$  (see Ref. [16]). They adopt simple forms in the low transparency case and for  $T = 1$ . In the tunnel regime one finds (for a symmetric junction)

$$P_n(T \ll 1) = \frac{T^n}{4^{n-1}} \rho_0 \rho_n \prod_{k=1}^{n-1} |f_k^A|^2, \quad (4)$$

where  $\rho(E)$  is the lead density of states, and  $\rho_n = \rho(E + neV)$ . With this expression one recovers the result of the multiparticle tunneling theory of Schrieffer and Wilkins<sup>3</sup>.

For perfect transparency ( $T = 1$ ), the absence of normal backscattering also simplifies the expressions of  $P_n(E, V)$ , which can be written as ( $n \geq 1$ )

$$P_n(T = 1) = \sum_{l=0}^{n-1} (1 - |a_{-n+l}|^2) \left[ \prod_{k=-n+l+1}^{l-1} |a_k|^2 \right] (1 - |a_l|^2), \quad (5)$$

where  $a(E)$  is the Andreev reflection coefficient defined as  $a(E) = -if^R(E)/[1 + g^R(E)]$ , and  $a_n = a(E + neV)$ . As can be seen in Eq. (5), a quasiparticle can only move upwards in energy

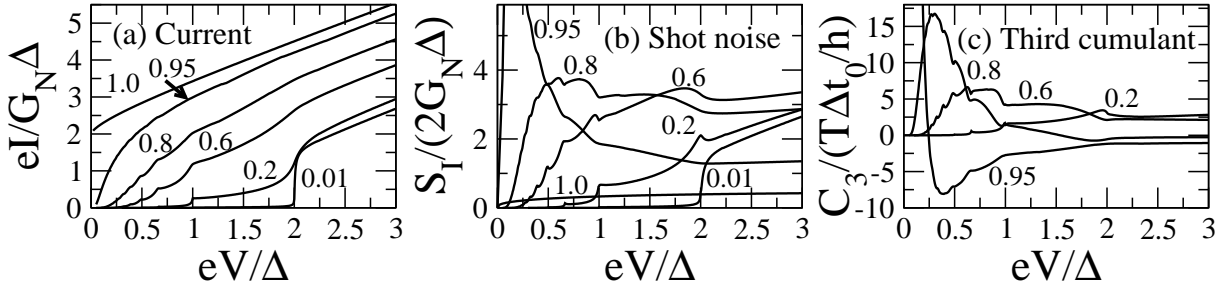


Figure 2: Current, shot noise and third cumulant at zero temperature as a function of the voltage for BCS superconductors of gap  $\Delta$ . The different curves correspond to different transmission coefficients as indicated in the panels. Here,  $G_N = (2e^2/h)T$  is the normal state conductance.

due to the absence of normal reflection. If we use this expression in the current formula we recover the result obtain by Klapwijk, Blonder and Tinkham<sup>4</sup> for  $T = 1$ .

### 2.3 Cumulants

From the CGF one can easily calculate the cumulants of the distribution and in turn many transport properties. Of special interest are the first three cumulants  $C_1$ ,  $C_2$  and  $C_3$ , which correspond to the average, width and skewness of the distribution, respectively. From Eq.(3) it follows that these cumulants can be expressed in terms of the probabilities  $P_n(E, V)$  as follows

$$\begin{aligned}
 C_1 &= \frac{t_0}{h} \int_0^{eV} dE \sum_n n P_n, & C_2 &= \frac{t_0}{h} \int_0^{eV} dE \left\{ \sum_n n^2 P_n - \left( \sum_n n P_n \right)^2 \right\}, \\
 C_3 &= \frac{t_0}{h} \int_0^{eV} dE \left\{ \sum_n n^3 P_n + 2 \left( \sum_n n P_n \right)^3 - 3 \left( \sum_n n P_n \right) \left( \sum_n n^2 P_n \right) \right\} \quad (6)
 \end{aligned}$$

These expressions are a simple consequence of the fact that the charge transfer distribution is multinomial in energy space. At zero temperature the sums over  $n$  are restricted to  $n \geq 1$ .

## 3 Transport properties of superconducting atomic point contacts

We analyze in this section the dc transport properties of point contacts between BCS superconductors with a gap  $\Delta$ , which is the situation realized in the metallic atomic-sized contacts.

In Fig. 2 we show the first three cumulants of the charge transfer distribution: current, shot noise and skewness (third cumulant). Let us discuss their most remarkable features. (i) The current exhibits the so-called subharmonic gap structure, as discussed in the introduction. This subgap structure evolves from a step-like behavior for low transmission to its disappearance at perfect transparency. (ii) The shot noise in the subgap region can be much larger than the Poisson noise ( $S_{I, Poisson} = 2eI$ ). Moreover, in the tunneling regime the effective charge defined as the ratio  $q \equiv S_I/2I$  is quantized in units of the electron charge:  $q(V)/e = 1 + \text{Int}(2\Delta/eV)$ . This is illustrated in Fig. 3, where the ratios  $C_2/C_1$  and  $C_3/C_1$  are shown as a function of the voltage. (iii) As shown in Fig. 3, the third cumulant at low transmissions is described by  $C_3 = q^2 C_1$ , where again  $q$  is the quantized effective charge defined above. For higher transmissions this cumulant is negative at high voltage as in the normal state, where  $C_3 = (t_0/h)T(1-T)(1-2T)eV$ , but it becomes positive at low bias, and after this sign change there is a huge increase.

The features described in the previous paragraph can be easily understood with the help of an analysis of the probabilities  $P_n(E, V)$ . To give an idea about them, in Fig. 4 we have plotted their

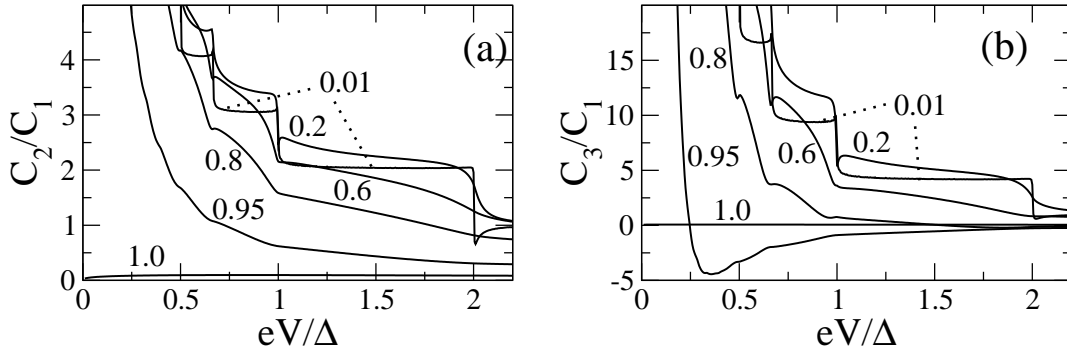


Figure 3: (a) Second cumulant and (b) third cumulant at zero temperature for BCS superconductors. Both are normalized to the first cumulant (the average current). The transmissions are indicated in the plots.

average value for two very different transmissions defined as  $\bar{P}_n(V) \equiv (1/eV) \int_0^{eV} dE P_n(E, V)$ . First of all, notice that, no matter what the transmission is, the probability of an  $n$ -order MAR has a threshold voltage  $eV_n = 2\Delta/n$ , below which the process is forbidden. When  $V > V_n$  an  $n$ -order MAR gives a new contribution to the transport, which is finally the explanation of the subharmonic gap structure. On the other hand, the big difference between the tunneling regime and perfect transparency can be explained as follows. At low transparency there are two factors that make the subgap structure so pronounced. First, at  $V_n$  the  $n$ -order MAR is a process that connects the two gap edges, where the BCS density of states diverges (see Eq.(4)). This fact, together of course with its higher probability, implies that this MAR rapidly dominates the shape of the I-V curves giving rise to a non-linearity at  $V_n$ . Second, at  $V_n$  there is a huge enhancement of the probabilities of the MARs of order  $m > n$ . This is due to the fact that precisely at  $V_n$  the MAR trajectories can connect both gap edges, which as can be seen in Eq. (4) increases enormously their probability. At perfect transparency, the MAR probabilities do not exhibit any abrupt feature (see Fig. 4b). This is due to the fact that the BCS density of states is renormalized, and in particular, the divergences disappear (see Eq.(5)). This fact explains naturally why the subharmonic gap structure is completely washed out at  $T = 1$ .

Another interesting feature of the MAR probabilities occurs at low transparencies. As one can see in Fig. 4a, at a voltage  $2\Delta/n < eV < 2\Delta/(n-1)$  the MAR of order  $n$  has a much higher probability than the other MARs. This means that in this voltage window the  $n$ -order MAR clearly dominates the transport properties and the charge is predominantly transferred in packets of  $ne$ . This fact explains the charge quantization in the tunnel regime observed both in  $C_2$  and  $C_3$  (see Fig. 3). More generally, this fact implies that at low transparencies the multinomial distribution of Eq.(3) becomes Poissonian, and in this limit all the cumulants are proportional to the current:  $C_n = (q(V)/e)^n C_1$ , where  $q(V)$  is the voltage-dependent quantized charge. When the transmission is not very low, there are always several MARs that give a significant contribution to the transport at every voltage (see Fig. 4b). This explains why the charge is in general not quantized.

The explanation for the sign change of  $C_3$  at low bias and high transparencies can be found in Eq. (6). In order to get a positive value for  $C_3$ , one needs the first two terms in Eq. (6) to dominate, which happens when  $P_n \ll 1$ . This is precisely what happens at low bias, where the MAR probabilities are rather small. On the other hand, the huge enhancement after the sign change is due to fact that  $n$ , the charge transferred by these MARs, is indeed huge a low bias.

Finally, at  $T = 1$  the cumulants  $C_n$  (with  $n > 1$ ) do not completely vanish due to the fact that at a given voltage different MARs give a significant contribution, and therefore their probability is smaller than one (see Fig. 4(b)).

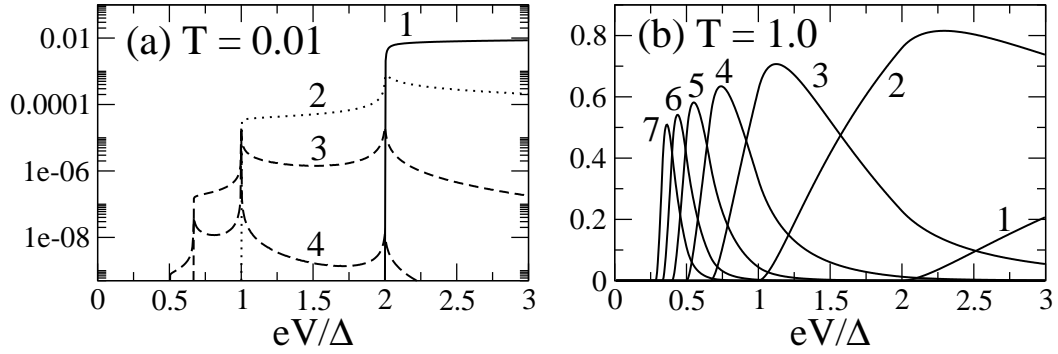


Figure 4: Average MAR probabilities  $\bar{P}_n(V) \equiv (1/eV) \int_0^{eV} dE P_n(E, V)$  as a function of voltage for a contact between BCS superconductors at zero temperature. The two panels correspond to two different transmissions. The index of the processes is indicated in the plots. Notice the logarithmic scale in the panel (a).

## Acknowledgments

We acknowledge discussions with A. Levy Yeyati, A. Martín-Rodero and Yu.V. Nazarov. JCC was financially supported by the DFG within the CFN and by the Helmholtz Gemeinschaft (contract VH-NG-029), and WB by the Swiss NSF and the NCCR Nanoscience.

## References

1. B.N. Taylor and E. Burstein, Phys. Rev. Lett. **10**, 14 (1963).
2. I.K. Yanson, V.M. Svistunov, and I.M. Dmitrenko, Sov. Phys. JETP **20**, 1404 (1965).
3. J.R. Schrieffer and J.W. Wilkins, Phys. Rev. Lett. **10**, 17 (1963).
4. T.M. Klapwijk, G.E. Blonder and M. Tinkham, Physica B **109&110**, 1657 (1982).
5. E.N. Bratus, V.S. Shumeiko, and G. Wendin, Phys. Rev. Lett. **74**, 2110 (1995).
6. D. Averin and A. Bardas, Phys. Rev. Lett. **75**, 1831 (1995).
7. J.C. Cuevas, A. Martín-Rodero and A. Levy Yeyati, Phys. Rev. B **54**, 7366 (1996).
8. J.C. Cuevas, A. Martín-Rodero and A. Levy Yeyati, Phys. Rev. Lett. **82**, 4086 (1999).
9. Y. Naveh and D.V. Averin, Phys. Rev. Lett. **82**, 4090 (1999).
10. J.C. Cuevas, J. Heurich, A. Martín-Rodero, A. Levy Yeyati, G. Schön, Phys. Rev. Lett. **88**, 157001 (2002).
11. N. van der Post, E.T. Peters, I.K. Yanson, and J.M. van Ruitenbeek, Phys. Rev. Lett. **73**, 2611 (1994).
12. E. Scheer, P. Joyez, D. Esteve, C. Urbina and M.H. Devoret, Phys. Rev. Lett. **78**, 3535 (1997).
13. E. Scheer, N. Agraït, J.C. Cuevas, A. Levy Yeyati, B. Ludoph, A. Martín-Rodero, G. Rubio, J.M. van Ruitenbeek and C. Urbina, Nature **394**, 154 (1998).
14. M.F. Goffman *et al.*, Phys. Rev. Lett. **85**, 170 (2000).
15. R. Cron *et al.*, Phys. Rev. Lett. **86**, 4104 (2001).
16. J.C. Cuevas and W. Belzig, Phys. Rev. Lett. **91**, 187001 (2003).
17. G. Johansson, P. Samuelsson and A. Ingerman, Phys. Rev. Lett. **91**, 187002 (2003).
18. L.S. Levitov and G.B. Lesovik, Pis'ma Zh. Eksp. Teor. Fiz. **58**, 225 (1993). L.S. Levitov, H.W. Lee, and G.B. Lesovik, J. Math. Phys. **37**, 4845 (1996).
19. *Quantum Noise in Mesoscopic Physics*, edited by Yu.V. Nazarov (Kluwer, Dordrecht, 2003).
20. Yu. V. Nazarov, Ann. Phys. (Leipzig) **8**, SI-193 (1999).
21. W. Belzig and Yu. V. Nazarov, Phys. Rev. Lett. **87**, 197006 (2001).